Studies on the pathogenesis of chronic kidney disease

He, J.

Chapter 5

Ctns mutant adult zebrafish develop nephropathic cystinosis

Junling He*, Sante Princiero Berlingerio*, Bert van den Heuvel, Hans J Baelde, Elena Levtchenko.

*These authors contributed equally to this work

Abstract

Cystinosis is a lysosomal storage disease caused by mutations of the *CTNS* gene encoding cystinosin. Defective cystinosin function results in the intralysosomal accumulation of cystine in all cells. Most patients with cystinosis have kidney disease presenting as generalized proximal tubular dysfunction (called renal Fanconi syndrome) followed by glomerular damage and progressing towards end-stage kidney failure. In our previous study, we generated a *ctns* mutant zebrafish that displayed glomerular and tubular dysfunction at the larval stage. In the current study, we further investigated the renal histopathology of *ctns* mutant zebrafish at the adult stage. We observed hyaline-like eosinophilic droplets and cytoplasmic vacuoles in the renal proximal tubular epithelial cells of *ctns* mutant adult zebrafish, in both genders, on HE- and PAS- stained slides, which were not present in controls. Additionally, we found that these cytoplasmic vacuoles have a rectangular or polymorphous shape on toluidine blue-stained slides and images captured by transmission electron microscopy. These findings indicate that cystine crystals, the hallmark of cystinosis, are present in the renal proximal tubular cells of *ctns* mutant adult zebrafish. Further, compared with controls, the *ctns* mutant adult zebrafish had glomerular hypertrophy and increased expression of cleaved caspase-3 in the renal proximal tubular cells. Collectively, our data indicate that the kidney pathology of *ctns* mutant adult zebrafish has features of human nephropathic cystinosis and might be a promising model for understanding the pathogenesis of nephropathic cystinosis.

Introduction

Cystinosis is a rare and incurable lysosomal storage disease. Mutations in the *CTNS* gene encoding cystinosin cause the defective lysosomal cystine transport [1,2], resulting in the intralysosomal accumulation of cystine in all cells and tissues. In most patients with cystinosis, the disease initially manifests in the kidney, being the most common cause of inherited renal Fanconi syndrome in humans [3]. Fanconi syndrome is a result of inadequate reabsorption of nutrients and minerals in the renal proximal tubule leading to losses of essential molecules and metabolism into the urine. The proximal tubular damage is followed by progressive glomerular dysfunction and, when left untreated, leads to end-stage kidney failure. The underlying mechanisms of nephropathic cystinosis are still incompletely understood, and current therapy with cystine depleting drug cysteamine is not curative [3]. Therefore, further understanding the pathogenesis of nephropathic cystinosis and finding new therapeutic options are urgently needed.

Although cystine accumulation is the crucial feature of cystinosis, numerous studies suggested the role of inflammation [4], oxidative stress [5,6] and altered cell death mechanisms (autophagy [7-9] and apoptosis [10,11]) in the development of kidney phenotype. To better understand the molecular mechanisms of a particular disease, a suitable animal model is needed. The first *Ctns*-/- mouse model was generated in a mixed 129Sv x C57BL/6 strain [12]. In this *Ctns*-/- mouse model, cystine accumulation was found in kidney, liver, and muscle tissues. However, these mice failed to develop renal proximal tubulopathy or glomerular dysfunction. Afterwards, Nevo and colleagues generated *Ctns*-/- mice on a C57BL/6 and FVB/N background [13]. They showed that *Ctns*-/- mice with C57BL/6 background had an accumulation of cystine in all studied tissues. Additionally, these *Ctns*-/- mice had pronounced histological renal lesions in the proximal tubules and eventually developed chronic renal failure. In contrast, the *Ctns*-/- mice with FVB/N background did not develop renal dysfunction. This finding indicated that the genetic background influences the renal phenotype in mice. Recently, Shimizu *et al*. established a novel congenic *Ctns*^{ugl} mutation in a rat strain with the F344 genetic background [14]. The F344-*Ctns* mutant rats developed remarkable renal lesions and showed the cystine crystals in the lysosomes of the kidney cortex.

The rodent models are commonly used to investigate human diseases with a lot of advantages. However, generating a new murine model are usually time-consuming and expensive. To date, zebrafish models become an attractive tool for investigating human diseases [15]. In a previous study, we generated a congenic zebrafish model (*ctns*-/-) with a homozygous nonsense mutation in the exon 8 of the *ctns* gene, resulting in a functional loss of cystinosin [16]. The *ctns* mutant

zebrafish larvae present with delayed development, cystine accumulation, and signs of pronephric glomerular and tubular dysfunction, which closely resemble the phenotype of human nephropathic cystinosis. Additionally, we found that eight-month-old adult zebrafish had 20-fold increased cystine levels in the kidney compared with controls. Until now, data of *ctns* mutant adult zebrafish are lacking. In the current study, we aim to characterize the *ctns* mutant adult zebrafish' renal features and compare them with the age-matched control adult zebrafish by performing histopathological examinations.

Methods and Materials

Animals

Zebrafish were handled in compliance with the local animal welfare regulations and maintained according to standard protocols (zfin.org). The details of generating the *ctns* mutant zebrafish were described in our previous study (11). For this study, we included *ctns* mutant zebrafish at 3 (female=3 and male=3), 6 (female=3 and male=3) and 18 (female=6 and male=6) months old and the age and sex-matched AB control zebrafish. This study was approved by the local animal welfare committee (DEC) of the University of Leuven (number of the project:142/2019).

HE & PAS staining

After zebrafish were sacrificed, the whole zebrafish were immediately fixed in 4% buffered paraformaldehyde (4% PFA) at 4ºC for 1 week. After being washed with PBS twice, the zebrafish were transferred to EDTA solution (100mM, pH=8) for the decalcification for another 1 week, followed by embedding into paraffin. Paraffin-embedded zebrafish tissue was cut (4-µm thickness) on a Leica microtome (Wetzlar). Sections were stained with hematoxylin and eosin (HE) and Periodic-acid Schiff (PAS) according to the standard protocols.

Immunohistochemistry (cleaved caspase-3 staining)

Sections with the fresh-cut zebrafish tissue were deparaffinized and rehydrated. For cleaved caspase-3 staining, sections were subjected to heat-induced antigen retrieval using 10mM citrate buffer (pH=6). After blocking with 5% Normal Goat Serum (NGS) in PBS, the sections were incubated with rabbit anti-cleaved caspase-3 (1:200, Cell Signaling Technology Europe, The Netherlands) followed by an anti-rabbit-Envision, HRP-labelled secondary antibody (Dako, Denmark). As a negative control, a normal rabbit serum was used instead of the primary antibody. Diaminobenzidine (DAB+; Dako, Denmark) was used as the chromogen. Subsequently, sections were counterstained with HE, dehydrated and mounted.

Toluidine blue staining and Transmission electron microscopy (TEM)

Zebrafish renal tissues were harvested and fixed in the EM fixation buffer (1,5% glutaraldehyde / 1% paraformaldehyde) for 24 hours. Subsequently, the renal tissues were post-fixed with 2.5% glutaraldehyde/1.2% acrolein in fixation buffer (0.1 mol/l cacodylate, 0.1 mol/l sucrose, pH 7.4) and 1% osmium tetroxide, and embedded into epon resin. Semi-thin sections (0.5-µm thickness) were stained with toluidine blue. The ultrathin sections were stained with uranyl acetate. The images were collected using a JEM-1200 EX transmission electron microscopy (JEOL, Tokyo, Japan) with different magnifications.

Digital image analysis

Stained slides were digitized using a Philips Ultra-Fast Scanner 1.6 RA (Philips Electronics). To analyze glomerular hypertrophy in zebrafish, the surface area (μm^2) of Bowman's capsule, Bowman's space, and glomerular tuft was measured on PAS-stained slides. All available glomeruli per section were included and measured using ImageJ software (https:// imagej.nih.gov/ij/). The average of the measurements from each zebrafish was used for statistical analyses.

Two observers scored the cleaved caspase-3 expression in the tubules of each zebrafish. The semiquantitative score was conducted on the three random chosen tubular fields in each fish (20X magnification). The percentage of caspase-3 positive area relative to the total area of tubules was scored as 1 (negative staining), 2 (1-10% positive staining), 3 (10%-25% positive staining), 4 (>25% positive staining). The mean of the score from each zebrafish was used for statistical analyses.

Statistical analyses

Statistical analysis was performed using SPSS (IBM, New York). Data of two groups was analyzed using Student's *t*-test. Differences with $P<0.05$ were considered as statistically significant.

Results

Ctns mutant zebrafish show renal proximal tubular damage

First, we examined the histological characteristics of renal tubules in control and *ctns* mutant adult zebrafish of both genders at 3, 6 and 18 months of age. Proximal tubules showed eosinophilic cytoplasm (dark pink cytoplasm) and brush borders which were easy to identify on HE-stained slides (Fig.1A and 1E). Distal tubules had less eosinophilic cytoplasm (light pink cytoplasm) on HE-stained slides (Fig.1A and 1E). In all control zebrafish, no structural changes were found in both proximal and distal tubules (Fig.1A, 1C, and 1E). However, we observed the histological alterations including cloudy swelling, hyaline-like eosinophilic droplets and cytoplasmic vacuoles in the renal proximal tubules of *ctns* mutant female and male zebrafish at all three ages (Fig. 1B, 1D, and 1F). Furthermore, the cytoplasmic vacuoles were more frequently observed in the renal proximal tubules of 18 months old *ctns* mutant zebrafish, compared to *ctns* mutant zebrafish of younger ages (Fig.1B,1D, and 1F).

On PAS-stained slides, we did not find any histological alterations in the tubules of control zebrafish (Fig.1G). The hyaline droplets and cytoplasmic vacuoles were only observed in the renal proximal tubules of *ctns* mutant zebrafish (Fig. 1H) on PAS-stained slides, which is in line with the findings on HE-stained slides.

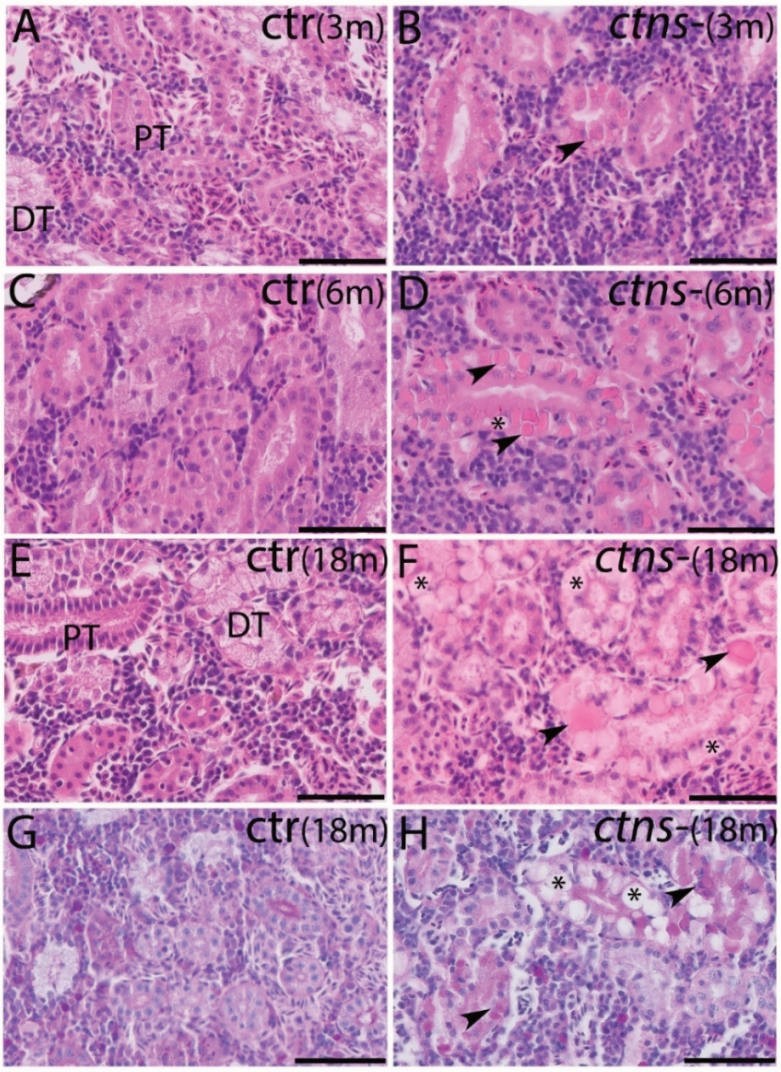

Figure 1. Cloudy swelling, hyaline-like eosinophilic droplets and cytoplasmic vacuoles in the renal proximal tubules of *ctns* mutant zebrafish

(A-B) Representative images of renal tubules of control (A) and *ctns* mutant (B) zebrafish at 3 months. Details of proximal tubules with hyaline-like eosinophilic droplets (black arrowhead). HE staining; the scale bars represent 50µm. (C-D) Representative images of renal tubules of control (C) and *ctns* mutant (D) zebrafish at 6 months. Details of proximal tubules with hyaline-like eosinophilic droplets (black arrowhead) and cytoplasmic vacuoles (*). HE staining; the scale bars represent 50µm. (E-F) Representative images of renal tubules of control (E) and *ctns* mutant (F) zebrafish at 18 months. Details of proximal tubules with hyaline-like eosinophilic droplets (black arrowhead) and cytoplasmic vacuoles (*). HE staining, the scale bars represent 50µm. (G-H) Representative images of the PAS staining of renal tubules of control (G) and *ctns* mutant (H) zebrafish at 18 months. Details of proximal tubules with hyaline-like droplets (black arrowhead) and cytoplasmic vacuoles (*). The scale bars represent 50µm. PT: proximal tubule; DT: distal tubule. ctr: control zebrafish; *ctns*-: *ctns* mutant zebrafish; 3m: 3 months old; 6m: 6 months old; 18m: 18 months old.

Male *ctns* mutant zebrafish show glomerular hypertrophy

Since the proximal tubular damage was most pronounced at the age of 18 months, glomerular histology was studied in detail at this age. The *ctns* mutant male zebrafish had significant enlargement of Bowman's capsule (Fig. 2B and 2C) and glomerular tuft (Fig. 2B and 2D), but not Bowman's space(Fig. 2B and 2E) when compared with control male zebrafish (Fig. 2A, 2C, 2D, and 2E). Moreover, the surface area of Bowman's capsule, glomerular tuft and Bowman's space was also larger in *ctns* mutant female zebrafish, compared with control female zebrafish (Fig.2C-2E). However, this difference did not reach statistical significance. No proliferation of mesangial cells or glomerulosclerosis were observed in both control or *ctns* mutant zebrafish.

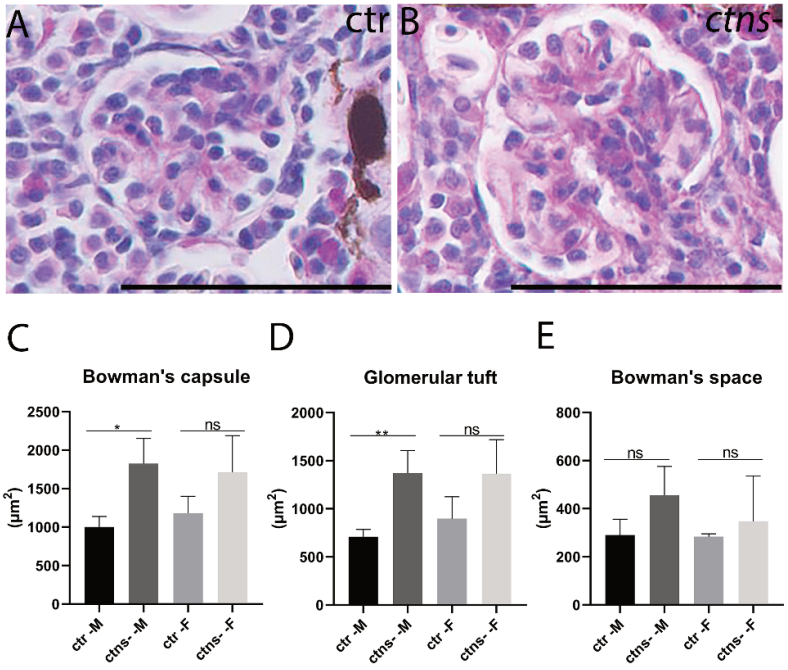

Figure 2. Male *ctns* mutant zebrafish have glomerular hypertrophy

(A-B) Representative images of the PAS staining of the glomerulus of control (A) and *ctns* mutant (B) zebrafish. The scale bars represent 50μm. (C-E) Summary of the surface areas of the Bowman's capsule (C), the glomerular tuft (D), and Bowman's space (E) of control and *ctns* mutant zebrafish in both genders (*P<0.05; **P<0.01; ns: no significance). ctr: control zebrafish, *ctns*-: *ctns* mutant zebrafish, M: male zebrafish, F: female zebrafish.

Cystine crystal accumulation in the renal proximal tubules of *ctns* mutant zebrafish

It has been reported that clear spaces reflecting dissolved crystals can be detected on toluidine blue-stained slides [17]. On toluidine blue-stained slides, we observed numerous cytoplasmic vacuoles with rectangular or polymorphous shape in the renal proximal epithelial cells of *ctns* mutant zebrafish (Fig. 3B and 3C), not controls (Fig. 3A). The rectangular or polymorphous shape of the cytoplasmic vacuoles is suggestive of the cystine crystals. We also found the nuclear fragmentation in the proximal tubular epithelial cells of *ctns* mutant zebrafish, indicating that apoptosis occurs in the proximal tubular epithelial cells of *ctns* mutant zebrafish (Fig. 3D).

Next, we examined the renal ultrastructure of control and *ctns* mutant zebrafish. We found the apical microvilli were intact in control zebrafish (Fig. 3E). However, a partial loss of brush borders and numerous cytoplasmic vacuoles were observed in the renal proximal tubules of *ctns* mutant zebrafish (Fig. 3F). The cytoplasmic vacuoles with rectangular or polymorphous shapes were also seen on the TEM images (Fig. 3F), suggesting the cystine crystals accumulation. On the TEM images, we did not observe the thickening of the glomerular basement membrane, podocyte foot process effacement, or abnormal fenestrated endothelial cells in the glomeruli of both control and *ctns* mutant zebrafish (Fig. 3G and 3H).

Apoptosis is involved in the pathogenesis of nephropathic cystinosis in zebrafish

Finally, we performed the cleaved caspase-3 staining on the renal tissues of control and *ctns* mutant zebrafish. We found that the cleaved caspase-3 expression was significantly increased in the renal proximal tubular cells of *ctns* mutant female and male zebrafish (Fig. 4G), compared with the control female and male zebrafish, in which the cleaved caspase-3 expression was almost negative in the renal proximal tubular cells (Fig. 4A and 4C). The expression of cleaved caspase-3 was mainly present in cells showing the cytoplasmic vacuoles (Fig. 4B and 4D), indicating that apoptosis takes place in the injured proximal tubules in *ctns* mutant zebrafish. The cleaved caspase-3 staining in glomeruli in both control and *ctns* mutant zebrafish, in both genders, was negative (Fig. 4E and 4F).

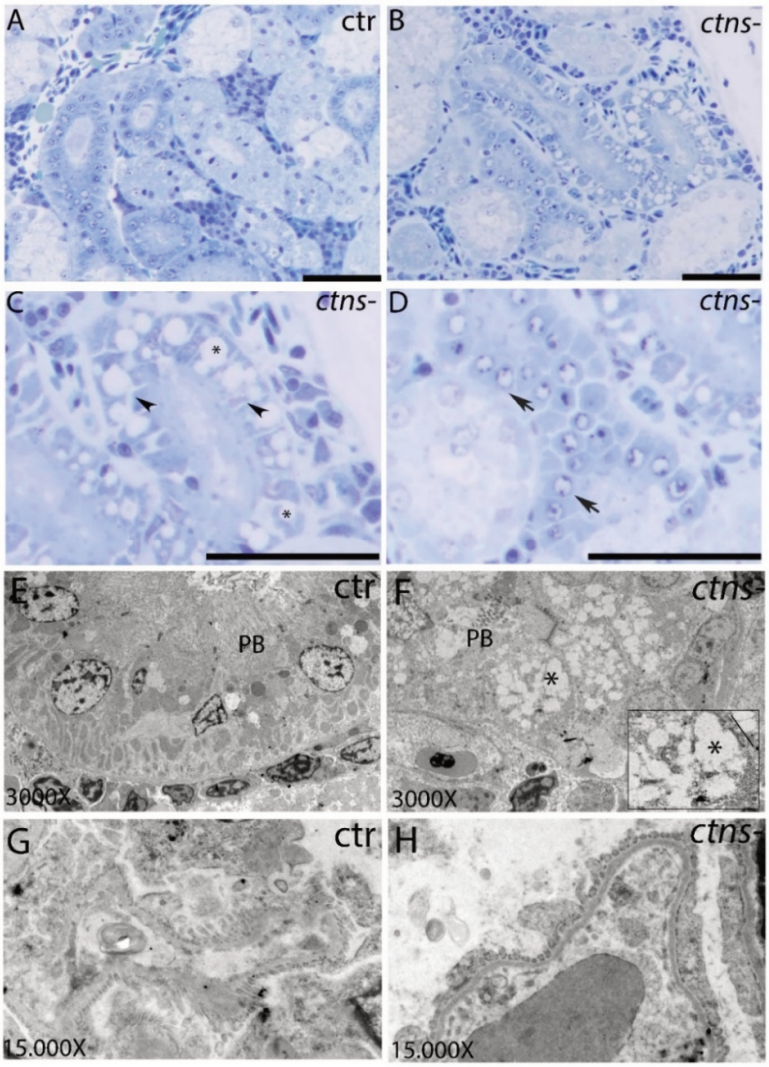

Figure 3. Presence of cytoplasmic vacuoles in the renal proximal tubules of *ctns* mutant zebrafish at 18 months

(A-B) Representative toluidine blue-stained images of renal proximal tubules in control (A) and *ctns* mutant (B) zebrafish. The scale bars represent 50µm. (C-D) Fig C and D show a higher magnification of Fig B. Details of renal proximal tubules with cytoplasmic vacuoles (C; *) and the rectangular and polymorphous vacuolar spaces (C; black arrowhead), and nuclear fragmentation (D; black arrow). (E-F) Representative TEM images of the renal proximal tubule of control (E) *ctns* mutant zebrafish (F). Partial loss of brush borders (PB) and an abundance of the rectangular and polymorphous vacuoles (*) were observed in the renal proximal tubule of *ctns* mutant zebrafish. The high-magnification view of the rectangle in the bottom right corner shows the polymorphous vacuoles and a large vacuole with straight membrane border segments (straight line); magnification 3000X. (G-H) Representative images of the glomerulus of control (G) and *ctns* mutant (H) zebrafish; magnification 15,000X. PB: proximal tubule brush border; ctr: control zebrafish, *ctns*-: *ctns* mutant zebrafish.

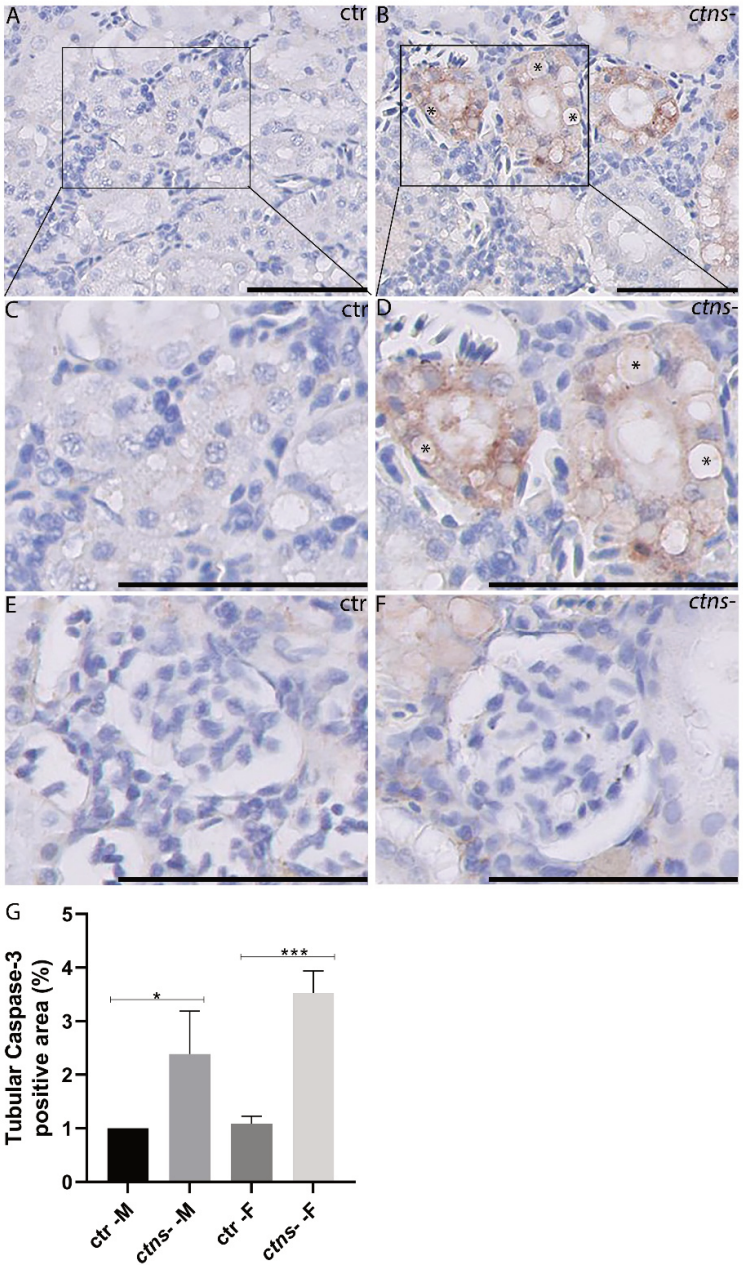

Figure 4. Apoptosis takes place in proximal tubular cells with vacuoles in *ctns* mutant zebrafish at 18 months

(A-B) Representative images of the cleaved caspase-3 immunostaining of tubules of control (A) and *ctns* mutant (B) zebrafish. The scale bars represent 50µm. (C-D) The bottom panels show a higher magnification of the boxed areas in the upper panels. Details of proximal tubular cells with cytoplasmic vacuoles (*); the scale bars represent 50µm. (E-F) Representative images of the cleaved caspase-3 immunostaining of glomerulus of control (E) and *ctns* mutant (F) zebrafish. The scale bars represent 50µm. (G) The summary of the tubular caspase-3 staining positive area in control and *ctns* mutant zebrafish (both female and male). (*P< 0.05, ***P<0.001). ctr: control zebrafish, *ctns*-: *ctns* mutant zebrafish, M: male, F: female.

Discussion

In the current study, the renal histopathology of *ctns* mutant zebrafish at the adult stage was investigated. We found numerous hyaline-like eosinophilic droplets, cytoplasmic vacuoles, and partial loss of brush borders in the proximal tubules of *ctns* mutant female and male zebrafish. We observed that the cytoplasmic vacuoles were in rectangular or polymorphous shape, indicating cystine crystals accumulation. We also found that *ctns* mutant male zebrafish developed glomerular hypertrophy. Lastly, we showed that cleaved-caspase 3 expression was significantly increased in the renal proximal tubular epithelial cells of *ctns* mutant female and male zebrafish, compared with controls, indicating that apoptosis is involved in the pathogenesis of nephropathic cystinosis in zebrafish.

Lysosomes are the sites of intracellular digestion that facilitate the degradation of foreign materials, and they are considered as the vital metabolic coordinators of cells [18]. Being a lysosomal storage disease, the key feature of cystinosis is the lysosomal cystine accumulation [12,19]. Previously, lysosomal swelling and hyaline-like eosinophilic droplets inside the lysosomes has been reported in cystine-loaded proximal tubules [20,21]. In the current study, the accumulation of hyaline-like eosinophilic droplets and cytoplasmic vacuoles in the proximal tubules was found in the *ctns* mutant zebrafish indicative for cystine accumulation and has been further confirmed by toluidine blue staining and electron microscopy.

In the human biopsies, cystine crystals are seen as clear spaces within interstitial macrophages and tubular epithelial cytoplasm [17]. Interestingly, in our previous study, cystine crystals were not detected in the *ctns* mutant zebrafish at the larval stage [16]. We suppose that tissue cystine crystallization is a cumulative process that needs time to develop. In the current study, we observed fewer cytoplasmic vacuoles in the renal proximal tubules at 3 months old *ctns* mutant zebrafish than at 18 months when the fish showed abundant cytoplasmic vacuoles having a rectangular or polymorphous shape in the renal proximal tubules. These findings are consistent with our previous study, which reported that 8 months old *ctns* mutant adult zebrafish had a 20-fold increase of cystine expression in the kidney than that of age-matched control zebrafish [16]. Aside from the cystine crystals accumulation in the lysosomes of the renal proximal tubules, multinucleated glomerular epithelial cells (particularly podocytes) and "swan neck" atrophy of tubular cells are the histopathological hallmarks of human renal disease in cystinosis [17]. However, in fish, we neither observe the multinucleated podocytes or the ‘swan neck’ deformity of the proximal tubules.

To assess the histological changes of the glomeruli of *ctns* mutant zebrafish, we measured the surface areas of Bowman's capsule, the glomerular tuft, and Bowman's space of *ctns* mutant

zebrafish on routine PAS-stained sections. We found that *ctns* mutant male zebrafish developed glomerular hypertrophy, which possibly related to hyperfiltration. However, no thickening of the glomerular basement membrane, podocytes foot process effacement, and abnormal fenestrated endothelial cells were found in the *ctns* mutant zebrafish of both genders. It has been well known that zebrafish has a unique ability to regenerate injured kidney [22], which might explain only mild glomerular damage. Taken together, we conclude that the primary renal lesion in *ctns* mutant zebrafish is the severe proximal tubulopathy.

Consistently with the previous study [16], we also observed a significantly increased cleaved caspase-3 expression and nuclear fragmentation in the proximal tubular epithelial cells of *ctns* mutant zebrafish. The expression of cleaved caspase-3 was mainly present in cells showing the cytoplasmic vacuoles, indicating that apoptosis takes place in the injured proximal tubules. It has been reported that lysosomal cystine release could activate protein kinase Cδ, resulting in stimulation of apoptosis in cultured renal proximal tubular epithelial cells [23]. Sumayao et al. demonstrated that excessive lysosomal cystine accumulation reduced glutathione levels which elevated intracellular reactive oxygen species production, and then disrupted the mitochondrial integrity and augmented apoptosis in the renal proximal tubular epithelial cells [6]. Due to the shortage of the materials, we could not investigate the precise mechanisms leading to apoptosis in these zebrafish, which should be further elucidated.

Nephropathic cystinosis, if untreated, will gradually progress to chronic renal failure. Aminothiol cysteamine is a standard therapy for cystinosis [24]. It can enter into the lysosomes and split the cystine molecule into cysteine and a cysteamine-cysteine mixed disulfide which can exit lysosomes bypassing the defective cystinosin. Cysteamine can prevent cystine accumulation and delays the disease's progression but cannot correct renal Fanconi syndrome [24,25]. As a lifelong treatment, cysteamine also has undesirable side effects. From this perspective, suitable animal models to test novel potential therapies are urgently needed. Our previous study demonstrated that *ctns* mutant larvae showed a significant decrease in cystine levels upon treatment with increasing concentrations of cysteamine [16]. In an experimental setting using zebrafish, drugs can be easily put into the water for testing the oral administration route. Hence, the *ctns* mutant zebrafish is a suitable and valuable animal model for exploring the pathogenesis and therapeutic strategies in cystinosis.

Acknowledgements

The first author, J. He was supported by the China Scholarship Council (CSC). We would like to thank Peter Neeskens for the technical support of transmission electron microscopy (TEM).

References

1 Town, M. *et al.* A novel gene encoding an integral membrane protein is mutated in nephropathic cystinosis. *Nat Genet* **18**, 319-324, doi:10.1038/ng0498-319 (1998).

2 Touchman, J. W. *et al.* The genomic region encompassing the nephropathic cystinosis gene (CTNS): complete sequencing of a 200-kb segment and discovery of a novel gene within the common cystinosis-causing deletion. *Genome Res* **10**, 165-173, doi:10.1101/gr.10.2.165 (2000).

3 Cherqui, S. & Courtoy, P. J. The renal Fanconi syndrome in cystinosis: pathogenic insights and therapeutic perspectives. *Nat Rev Nephrol* **13**, 115-131, doi:10.1038/nrneph.2016.182 (2017).

4 Prencipe, G. *et al.* Inflammasome activation by cystine crystals: implications for the pathogenesis of cystinosis. *J Am Soc Nephrol* **25**, 1163-1169, doi:10.1681/ASN.2013060653 (2014).

5 Galarreta, C. I. *et al.* The swan-neck lesion: proximal tubular adaptation to oxidative stress in nephropathic cystinosis. *Am J Physiol Renal Physiol* **308**, F1155-1166, doi:10.1152/ajprenal.00591.2014 (2015).

6 Sumayao, R., McEvoy, B., Newsholme, P. & McMorrow, T. Lysosomal cystine accumulation promotes mitochondrial depolarization and induction of redox-sensitive genes in human kidney proximal tubular cells. *J Physiol* **594**, 3353-3370, doi:10.1113/JP271858 (2016).

7 Ivanova, E. A. *et al.* Altered mTOR signalling in nephropathic cystinosis. *J Inherit Metab Dis* **39**, 457-464, doi:10.1007/s10545-016-9919-z (2016).

8 Sansanwal, P. & Sarwal, M. M. Abnormal mitochondrial autophagy in nephropathic cystinosis. *Autophagy* **6**, 971-973, doi:10.4161/auto.6.7.13099 (2010).

9 Sansanwal, P. *et al.* Mitochondrial autophagy promotes cellular injury in nephropathic cystinosis. *J Am Soc Nephrol* **21**, 272-283, doi:10.1681/ASN.2009040383 (2010).

10 Taranta, A. *et al.* Cystinosin-LKG rescues cystine accumulation and decreases apoptosis rate in cystinotic proximal tubular epithelial cells. *Pediatr Res* **81**, 113-119, doi:10.1038/pr.2016.184 (2017).

11 Park, M., Helip-Wooley, A. & Thoene, J. Lysosomal cystine storage augments apoptosis in cultured human fibroblasts and renal tubular epithelial cells. *J Am Soc Nephrol* **13**, 2878-2887, doi:10.1097/01.asn.0000036867.49866.59 (2002).

12 Cherqui, S. *et al.* Intralysosomal cystine accumulation in mice lacking cystinosin, the protein defective in cystinosis. *Mol Cell Biol* **22**, 7622-7632, doi:10.1128/mcb.22.21.7622-7632.2002 (2002).

13 Nevo, N. *et al.* Renal phenotype of the cystinosis mouse model is dependent upon genetic background. *Nephrol Dial Transplant* **25**, 1059-1066, doi:10.1093/ndt/gfp553 (2010).

14 Shimizu, Y. *et al.* A deletion in the Ctns gene causes renal tubular dysfunction and cystine accumulation in LEA/Tohm rats. *Mamm Genome* **30**, 23-33, doi:10.1007/s00335-018-9790-3 (2019).

15 Dooley, K. & Zon, L. I. Zebrafish: a model system for the study of human disease. *Curr Opin Genet Dev* **10**, 252-256, doi:10.1016/s0959-437x(00)00074-5 (2000).

16 Elmonem, M. A. *et al.* Cystinosis (ctns) zebrafish mutant shows pronephric glomerular and tubular dysfunction. *Sci Rep* **7**, 42583, doi:10.1038/srep42583 (2017).

17 Lusco, M. A., Najafian, B., Alpers, C. E. & Fogo, A. B. AJKD Atlas of Renal Pathology: Cystinosis. *Am J Kidney Dis* **70**, e23-e24, doi:10.1053/j.ajkd.2017.10.002 (2017).

18 Saftig, P. & Klumperman, J. Lysosome biogenesis and lysosomal membrane proteins: trafficking meets function. *Nat Rev Mol Cell Biol* **10**, 623-635, doi:10.1038/nrm2745 (2009).

19 Raggi, C. *et al.* Dedifferentiation and aberrations of the endolysosomal compartment characterize the early stage of nephropathic cystinosis. *Hum Mol Genet* **23**, 2266-2278, doi:10.1093/hmg/ddt617 (2014).

20 Hard, G. C. Some aids to histological recognition of hyaline droplet nephropathy in ninety-day toxicity studies. *Toxicol Pathol* **36**, 1014-1017, doi:10.1177/0192623308327413 (2008).

21 Sakarcan, A., Timmons, C. & Baum, M. Intracellular distribution of cystine in cystine-loaded proximal tubules. *Pediatr Res* **35**, 447-450 (1994).

22 Kroeger, P. T., Jr. & Wingert, R. A. Using zebrafish to study podocyte genesis during kidney development and regeneration. *Genesis* **52**, 771-792, doi:10.1002/dvg.22798 (2014).

23 Park, M. A., Pejovic, V., Kerisit, K. G., Junius, S. & Thoene, J. G. Increased apoptosis in cystinotic fibroblasts and renal proximal tubule epithelial cells results from cysteinylation of protein kinase Cdelta. *J Am Soc Nephrol* **17**, 3167-3175, doi:10.1681/ASN.2006050474 (2006).

24 Brodin-Sartorius, A. *et al.* Cysteamine therapy delays the progression of nephropathic cystinosis in late adolescents and adults. *Kidney Int* **81**, 179-189, doi:10.1038/ki.2011.277 (2012).

25 Gahl, W. A., Balog, J. Z. & Kleta, R. Nephropathic cystinosis in adults: natural history and effects of oral cysteamine therapy. *Ann Intern Med* **147**, 242-250, doi:10.7326/0003-4819-147-4-200708210-00006 (2007).